Weldability of Newly Developed Austenitic Alloys for Cryogenic Service: Part II—High-Nitrogen Stainless Steel Weld Metal

Yield and tensile strengths at cryogenic temperatures increased as the weld nitrogen content increased

BY T. OGAWA AND T. KOSEKI

ABSTRACT. The metallography, mechanical properties at 77 K (−320°F), and hot cracking susceptibility of different nitrogen-bearing austenitic stainless steel weld metals deposited with the GTAW process were studied. Determining the feasibility of using nitrogen-strengthened stainless steel as a weldable structural material at cryogenic temperatures was one of the goals of the investigation. Emphasis was placed on evaluating the effect of factors such as nitrogen content, solidification mode and ferrite content on the weld metallurgy.

Through metallographic analysis of the weld metal, the role of nitrogen in controlling the solidification mode was investigated. A nitrogen coefficient of 18 was determined as the nickel equivalent expression. The austenitizing effect of nitrogen at the initial stage of solidification was small when compared to the solid-state stage after solidification. A modified nickel equivalent was proposed to describe the solidification mode of the weld metal, while the ferrite content was well predicted by the DeLong diagram.

Both increased nitrogen content and ferrite number degraded the impact toughness but improved the strength of the weld metal at 77 K. The primary ferrite solidification mode also deteriorated the weld impact toughness to a great extent. The degradation of impact toughness with nitrogen was due to both solid-solution strengthening and precipitation of nitrogen. As for the resistance to hot cracking of the weld metal, reducing impurity levels and ferrite content were definitely beneficial, while reducing nitrogen seemed to have little effect.

Based on the results, fundamental rules for weld composition and metallurgical factors were proposed to attain the combination of cryogenic properties and integrity of the weld metal desired.

T. OGAWA is a Senior Researcher and T. KOSEKI is on the research staff at the Welding Technology Laboratory, Nippon Steel Corp., Sagamihara Kanagawa, Japan.

Paper sponsored by the National Bureau of Standards and presented at the AWS 67th Annual Meeting, held April 13–18, 1986, in Atlanta, Ga. Part I of this article appeared in the November 1987 Welding Journal.

Introduction

In recent years, nitrogen alloying has been extensively investigated for austenitic stainless steels and their weld metals. One of the major applications of nitrogen-bearing stainless steels is for cryogenic service as a structural material, because nitrogen, particularly, improves cryogenic strength as a solid-solution strengthener (Refs. 1–3 and 42). For instance, in large superconducting magnet systems for fusion energy reactors, structural materials are required to possess high strength and fracture toughness at 4 K, the operating temperature, because of the enormous forces in the magnet and limited space available for the structure (Ref. 4). From the standpoint of the best combination of cryogenic strength and toughness, nitrogen-bearing austenitic stainless steels are promising materials to meet the requirements (Ref. 5).

KEY WORDS

Austenitic Alloys
Cryogenic Service
Nitrogen Strength'ng
Stainless Steel
Japanese Research
Reduced Hot Cracking
Impact Toughness
Nitrogen Austenitizer
Solidification Modes
Ferrite Effects

Since the fabrication of the load-bearing members for such cryogenic systems requires welding of thick sections, the nitrogen-bearing austenitic stainless steels need to be weldable, with the weldments displaying high performance and integrity at cryogenic service temperature. Several researchers (Refs. 6–10) have investigated the weldability of nitrogen-bearing austenitic stainless steels, but only limited data are available as to cryogenic properties, and some effects of nitrogen remain poorly understood.

It has been shown by previous studies that austenitic stainless steel weld metal exhibits different solidification modes, and ferrite distribution and content are strongly dependent on the compositions (Refs. 11–16). These metallurgical factors remarkably influence weldability (Refs. 17–20). A typical example can be seen in the hot cracking tendency of the welds. Early studies (Refs. 21–23) found that increased ferrite content reduces hot cracking susceptibility of the welds, and more recent studies (Refs. 24, 25) have indicated that the primary delta ferrite solidification mode can attain higher resistance to hot cracking than the primary austenite solidification mode. As far as conventional 300-series stainless steel weld metals are concerned, solidification modes are well described on the basis of the Fe-Cr-Ni ternary diagram, and the amount of delta ferrite is successfully predicted by the DeLong diagram (Ref. 26), using the chromium and nickel equivalent. But as to the weld metal containing a higher amount of nitrogen and/or manganese, such description and prediction were found to be inaccurate, and other suitable expressions or equivalents for them have been sought and developed. Suutala (Ref. 27) stated that the solidification mode of austenitic stainless steel weld metal containing up to 0.23% nitrogen can be described using Hammer's equivalents (Ref. 28), but the ferrite content can be predicted by the DeLong

diagram. On the contrary, Okagawa (Ref. 29) reported that in nitrogen-added Type 304 welds, the nitrogen effect on ferrite content was smaller than that predicted by DeLong, and he estimated the nitrogen coefficient for nickel equivalent expression as 13.4, which was considerably lower than the coefficient of 30 determined by DeLong. Espy (Ref. 9) stated that the nitrogen effect as an austenitizer decreased as nitrogen content increased, and proposed the modified Schaeffler diagram, in which the nitrogen coefficient varied from 30 to 20 with nitrogen content. The discrepancies in the nitrogen effect result in a serious drawback in developing proper weld compositions that obtain the desired ferrite content and distribution.

The present investigation considers the nitrogen effect on the solidification mode and ferrite content of austenitic stainless steel weld metal, and relates it to such weld performances as cryogenic toughness, strength and hot cracking susceptibility.

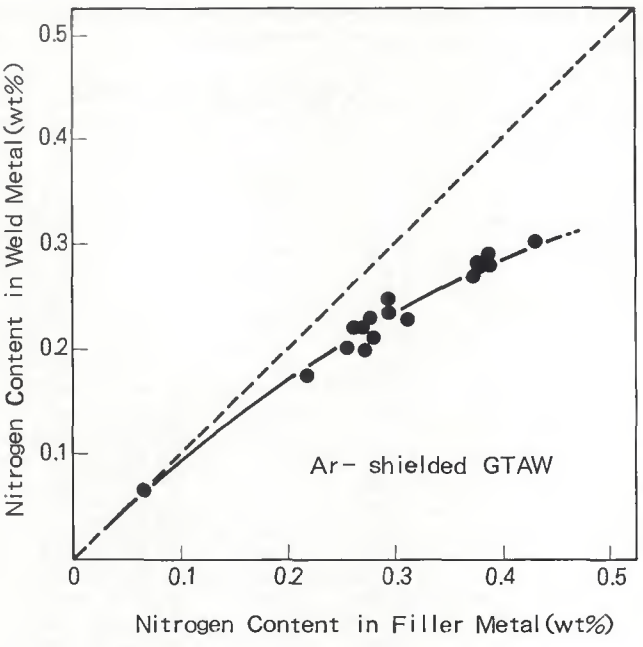

Fig. 1—Decrease of nitrogen content in argon-shielded GTA weld metals

Experimental Procedures

Different types of nitrogen-bearing austenitic stainless steel filler metals were made from laboratory-produced 50-kg (110-lb) heats that contained 25% chromium and varying amounts of nickel, manganese and nitrogen. In every heat, carbon content was reduced to less than 0.03 wt-% to minimize the low-temperature embrittlement caused by carbide precipitation (Refs. 17, 30). Sulfur and phosphorus contents were also reduced to the lowest possible levels to minimize hot cracking during welding (Ref. 23). All welds tested were made by gas tungsten arc welding (GTAW). The assemblies prepared were single-V (45-deg included angle) with a 6-mm (0.236-in.) root opening, machined from 12.7-mm (½-in.) thick plates having a composition of 25Cr-13Ni-1Mo-0.35N. Welding was carried out for all runs at a welding current of 200 A and a speed of 15 cm/min (5.9 ipm), with an interpass temperature of less than 150°C (302°F) and a heat input of 10.4 to 12 kJ/cm (26.4 to 30.5 kJ/in.). Pure argon was used as a shielding gas, but additionally, a mixture of Ar-2%N_2 was used for some of the filler metals to increase the weld nitrogen content.

Metallographic analysis was performed on all weld metals. Weld microstructure was examined by optical microscopy and transmission electron microscopy (TEM). Samples for optical microscopy were etched in a solution of 30% hydrochloric acid/50% nitric acid/20% water, or electrolytically etched in 50% nitric acid aqueous solution. Foils for TEM were prepared by jet-polishing with a 5% perchloric acid/glacial acetic acid solution. Electron probe microanalysis (EPMA) was performed to study concentration profiles of alloying elements in the weld metal by the line scanning technique. Precipitates were extracted electrolytically and identified by x-ray diffraction analysis. Retained delta ferrite content in the weld metal was measured with a permeability meter. The tabulated value is the average of more than five measurements around the undiluted weld metal center.

Charpy impact and tensile tests on the weld metals were performed at 77 K (−320°F). Standard size, 10- × 10- × 55-mm (0.394- × 0.394- × 2.165-in.), Charpy V-notch (CVN) specimens were extracted transverse to the welding direction, with the notch positioned at the center part of the weld metal normal to the weld surface. The fracture surfaces and their profiles of CVN specimens tested were examined by SEM and optical microscopy, respectively. Tensile specimens were 6 mm (0.234 in.) in diameter, with a 25-mm (0.984-in.) gage length, and extracted along the weld such that the entire specimen was all-weld metal. Reported data are the average of more than four values for impact toughness and more than two values for strength.

The Varestraint test was conducted to examine the hot cracking susceptibility of the weld metal. Test specimens were made from some of the above-mentioned heats and additional melted ones. Autogenous GTAW was carried out on 5-mm (0.2-in.) thick test specimens, at 70 A, traveling at 7.5 cm/min (2.95 ipm), with pure argon shielding gas. The augmented strain employed was 2.4%. Both the number and length of weld cracking were measured on as-tested weld surfaces under 30X and 60X magnification, and the ferrite content was also measured. The nitrogen content of the Varestraint-tested welds was analyzed by extracting a small pad from the weld.

Test Results

Metallography

The chemical compositions of the deposited weld metal studied are listed in Table 1. The A-series welds were made by Ar-shielded GTAW and the N-series by Ar/N_2-shielded GTAW. The nitrogen content of the weld metal was lower than that of the filler metals except for one weld (A16), as shown in Fig. 1.

The weld metals were classified into two main solidification modes according to the microstructures and EPMA results (Refs. 11–16), *i.e.*, primary ferrite solidification mode, hereafter referred to as FA mode (Ref. 13), and primary austenite solidification mode. The major mode in microstructure was employed when the weld metal showed a mixed mode. The welds that solidified as primary austenite were classified into two categories, *i.e.*, fully austenitic solidification mode and duplex solidification mode, hereafter referred to as A mode and AF mode, respectively (Ref. 12), which is important from a microstructural standpoint. The solidification mode and ferrite content of the weld metal are also given in Table 1.

The microstructure of the weld metal consisted of a cellular or cellular dendritic substructure, and the effect of nitrogen was not observed on the morphology and spacing of the substructure within the same solidification mode. Figure 2 shows typical microstructures observed for each solidification mode. The A mode, leading to a fully austenitic micro-

Table 1—Chemical Compositions, Solidification Mode and Measured Ferrite Content of the Weld Metals Studied

Weld ID	Chemical Composition (wt-%)								Solidification Mode[a]	Ferrite Content (measured) (%)
	C	Si	Mn	P	S	Cr	Ni	N		
A1	0.017	0.35	2.99	0.007	0.004	24.9	9.6	0.279	FA	8.8
A2	0.017	0.35	2.92	0.007	0.003	25.0	10.7	0.278	FA	6.7
A3	0.016	0.35	2.69	0.006	0.003	25.0	11.3	0.287	FA	5.2
A4	0.014	0.33	2.39	0.005	0.003	25.5	12.5	0.306	AF	3.5
A5	0.016	0.35	2.63	0.007	0.002	24.5	14.3	0.271	A	0
A6	0.014	0.36	2.70	0.005	0.004	24.9	16.8	0.281	A	0
A7	0.016	0.35	2.37	0.004	0.002	24.9	13.3	0.231	AF	3.0
A8	0.013	0.33	2.39	0.002	0.002	25.7	14.1	0.200	FA(+AF)	5.3
A9	0.015	0.41	3.95	0.009	0.005	24.8	14.4	0.221	AF	1.2
A10	0.018	0.38	4.13	0.009	0.005	25.4	15.4	0.212	AF	0.2
A11	0.017	0.37	5.29	0.008	0.005	24.8	15.1	0.236	A	0
A12	0.015	0.37	5.03	0.009	0.005	24.2	17.7	0.224	A	0
A13	0.014	0.32	2.53	0.004	0.001	24.1	17.7	0.223	A	0
A14	0.013	0.42	2.58	0.002	0.002	25.4	27.6	0.193	A	0
A15	0.012	0.30	2.66	0.004	0.002	24.0	20.3	0.169	A	0
A16	0.011	0.31	2.64	0.003	0.002	25.0	22.7	0.084	A	0
A17	0.029	0.27	6.75	0.007	0.003	20.4	16.0	0.247	A	0
N1	0.018	0.40	2.82	0.008	0.003	24.7	9.9	0.382	AF(+FA)	1.6
N2	0.019	0.38	2.78	0.007	0.003	24.6	10.5	0.390	AF	0.5
N3	0.017	0.38	2.57	0.008	0.003	24.9	11.4	0.403	A	0
N4	0.016	0.40	2.26	0.008	0.003	25.9	12.8	0.429	A	0
N5	0.017	0.37	2.57	0.008	0.002	24.7	14.4	0.367	A	0
N6	0.015	0.38	2.66	0.007	0.003	25.0	16.8	0.374	A	0

(a) FA – primary ferrite solidification.
AF – primary austenite solidification with eutectic-ferrite formation at terminal transient stage.
A – single-phase austenite solidification.

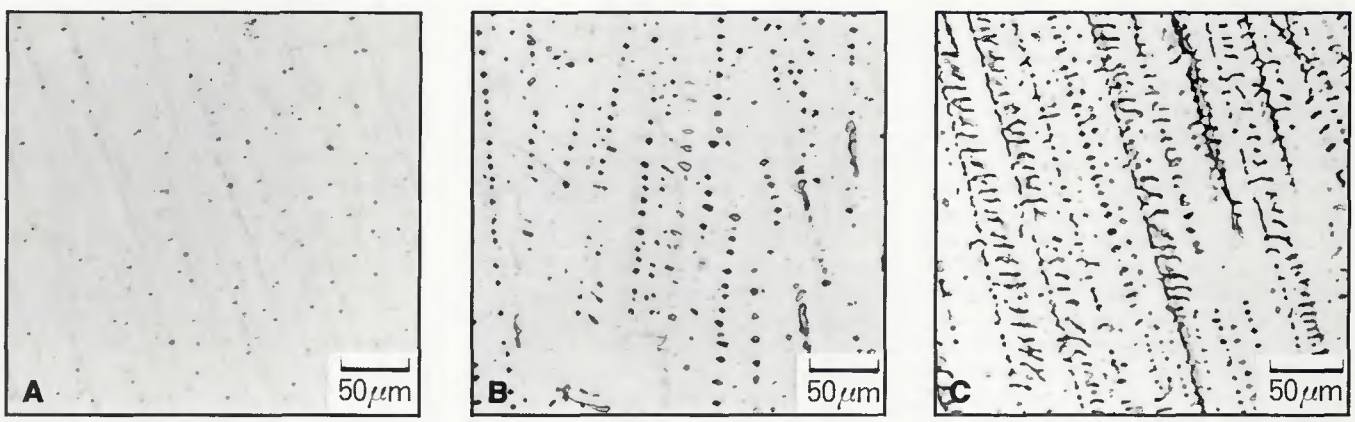

Fig. 2 – Typical microstructure of the weld metals observed for each solidification mode. A – The A mode (Weld No. A6); B – the AF mode (Weld No. A4); C – the FA mode (Weld No. A2)

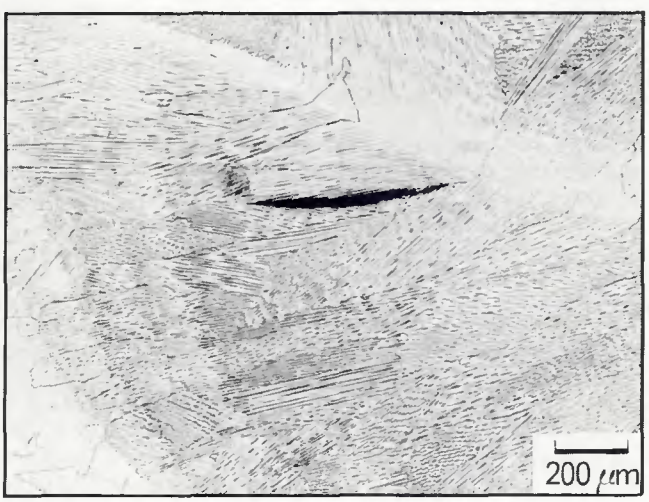

Fig. 3 – Typical microfissure observed in A-mode (fully austenitic) weld metal (Weld No. A6)

structure, showed no indications of delta ferrite formation during solidification, while the AF mode showed "vermicular" (Ref. 12) morphology of eutectic ferrite at intercellular regions. In some A-mode weld metals, microfissures were occasionally observed along austenitic grain boundaries, as shown in Fig. 3. The FA mode led to a duplex microstructure with a "skeletal" (Ref. 16) ferrite morphology at the cores of cellular dendrites. Nitrogen was certainly the austenitizer, because increased nitrogen content altered the solidification mode from FA to AF or A and decreased the ferrite content in welds N1 to N3. Concentration profiles of major alloying elements across the substructures are shown for each mode in Fig. 4. In a fully austenitic weld (A

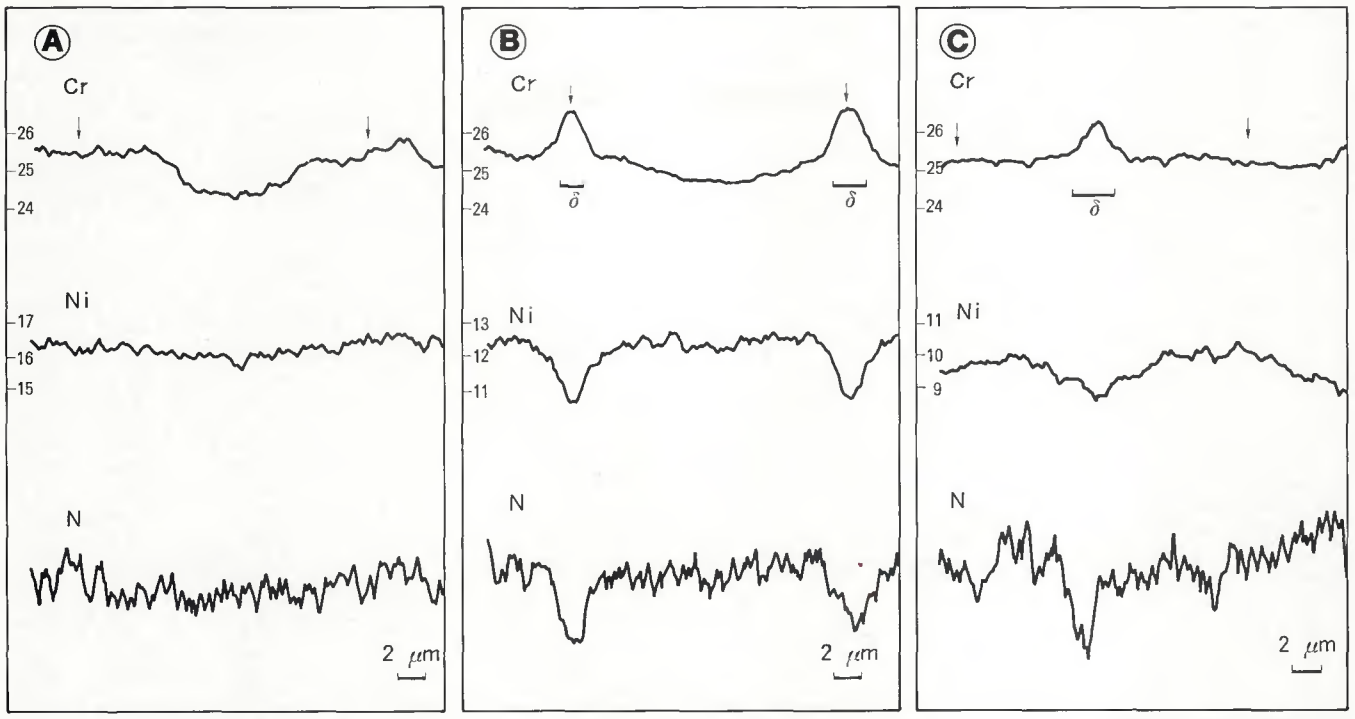

Fig. 4 — Concentration profiles of Cr, Ni and N across subgrains for each solidification mode. A — The A mode (Weld No. A6); B — the AF mode (Weld No. A4); C — the FA mode (Weld No. A2)

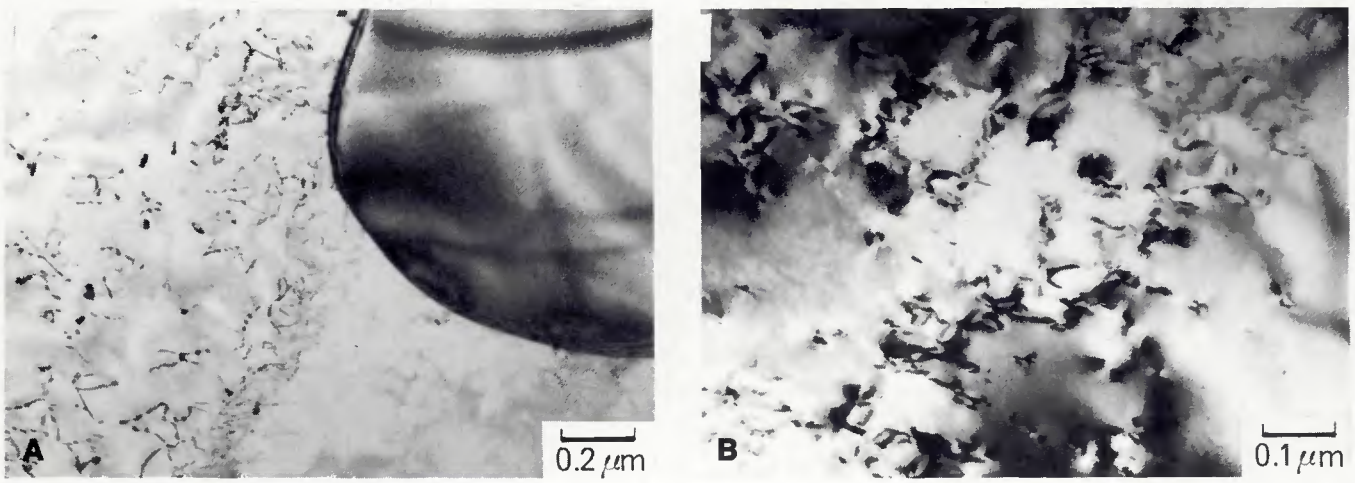

Fig. 5 — TEM micrographs of fine precipitates in austenite for: A — Weld No. A7; B — Weld No. A12

mode), both chromium and nickel were enriched at the intercellular regions. In a duplex weld (AF and FA mode), chromium was enriched and nickel was depleted in a ferritic matrix, and chromium was depleted and nickel was enriched in an austenitic matrix. In every mode, the concentration of manganese was the same manner as that of nickel. The difference of profiles between AF-mode and FA-mode weld metal was due to the different location of delta ferrite. Note that nitrogen was depleted in delta ferrite.

The precipitations such as chromium nitride and carbonitride were identified in every solidification mode weld by the x-ray diffraction analysis, though their peaks were rather weak. Through TEM analysis, fine precipitates with a size less than 0.1 μm were observed occasionally in austenite, as shown in Fig. 5, but seldom at ferrite-austenite interfaces.

Mechanical Properties at 77 K (−320°F)

Mechanical properties of the weld metals at 77 K (−320°F) are summarized in Table 2. The weld metals showed no indication of ferromagnetic martensite formation after mechanical tests at 77 K.

Figure 6 gives the effect of nitrogen and solidification mode on the weld impact toughness at 77 K. The impact toughness was degraded with weld nitrogen content. Primary ferrite solidification mode, the FA mode, considerably deteriorated the impact toughness. As for the weld metal solidifying as primary austenite, AF-mode weld metal exhibits slightly lower toughness than A-mode, fully austenitic weld metal. Figure 7 shows the typical SEM micrographs of the Charpy-impact fractured surface for each solidification mode. Both A- and AF-mode weld metal had completely ductile fracture surfaces, exhibiting the dimple pattern. On the other hand, FA-mode weld metal usually exhibited a mixture of ductile and

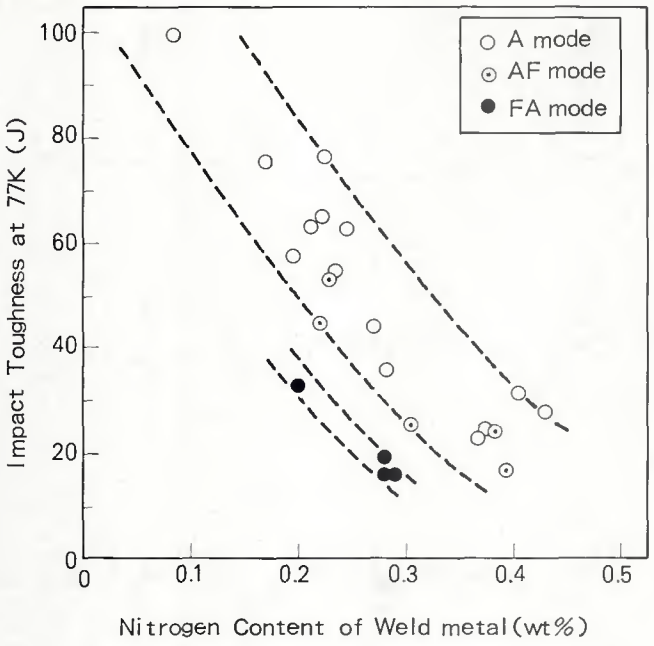

Fig. 6—Effect of nitrogen and solidification mode on the impact toughness of weld metal at 77 K (−320°F)

Table 2—Mechanical Properties of the Weld Metals at 77 K (−320°F)

Weld ID	Impact Toughness 77 K (−320°F) CVN Energy (J)	Tensile Properties at 77 K (−320°F) UTS (MPa)	0.2% YS (MPa)
A1	15.7	1566	1289
A2	19.6	1580	1268
A3	15.7	1613	1303
A4	25.5	1527	1230
A5	44.1	1263	1030
A6	34.3	1230	1051
A7	53.0	1404	1027
A8	32.4	1442	1032
A9	42.2	1298	1022
A10	62.8	1285	971
A11	54.9	1264	971
A12	76.5	1162	916
A13	64.7	1267	953
A14	56.9	1181	855
A15	75.5	1220	921
A16	100.0	1073	751
A17	62.8	–	–
N1	24.5	1667	1367
N2	16.8	1645	1274
N3	31.4	1663	1294
N4	28.4	–	–
N5	22.6	1353	1134
N6	24.5	–	–

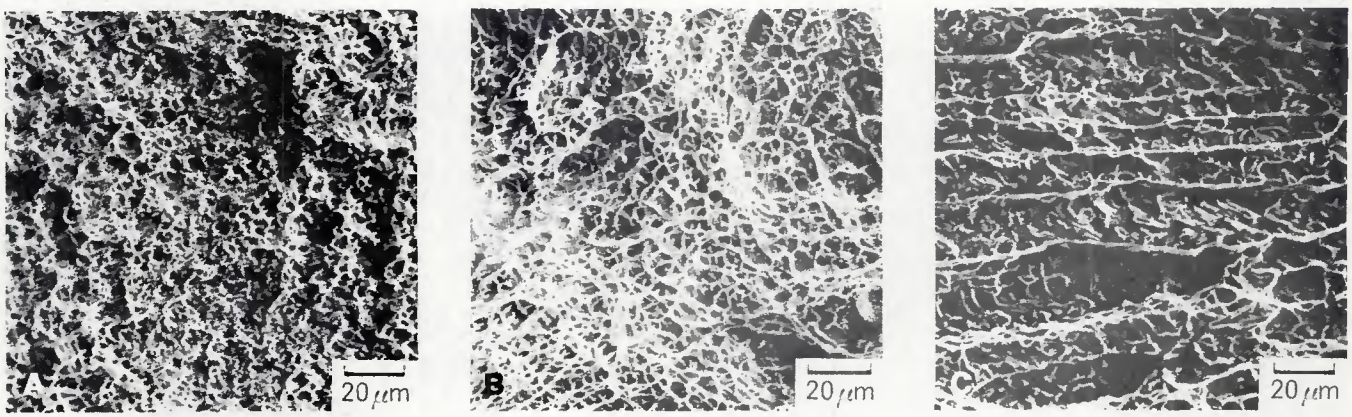

Fig. 7—Typical SEM micrograph of the 77 K CVN impact fracture surfaces for each solidification mode. A—The A mode (Weld No. A6); B—the AF mode (Weld No. A4); C—the FA mode (Weld No. A1)

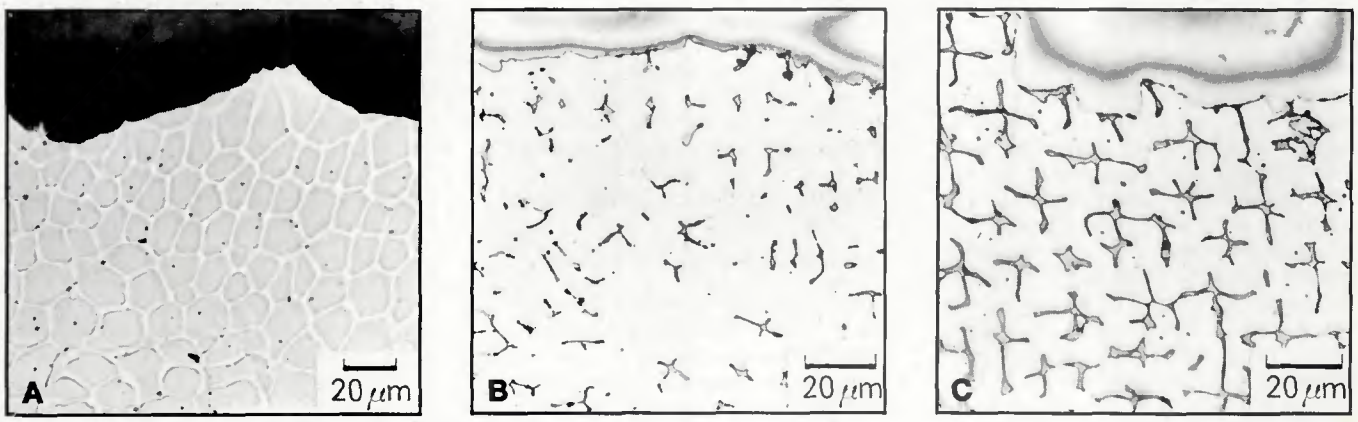

Fig. 8—Typical fracture surface profile of the 77 K CVN impact specimens for each solidification mode. A—The A mode (Weld No. A6); B—the AF mode (Weld No. A4); C—the FA mode (Weld No. A2)

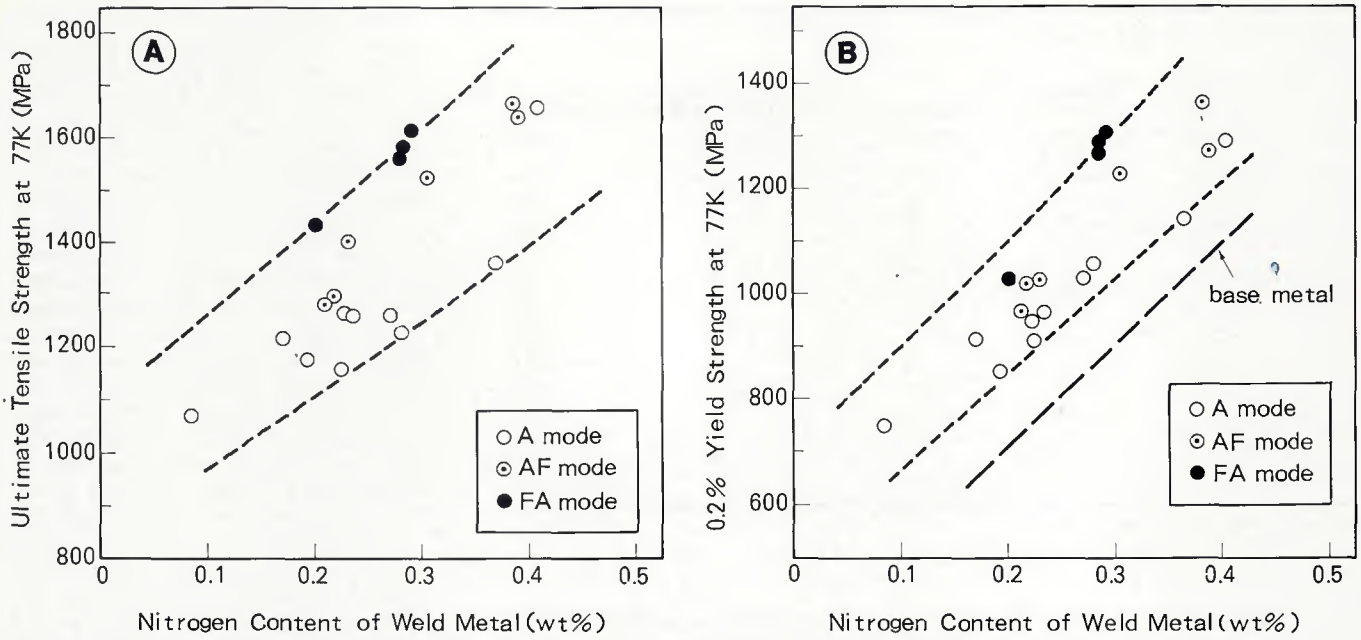

Fig. 9—Effect of nitrogen on the strength of weld metal at 77 K. A—Ultimate tensile strength; B—0.2% yield strength

brittle fracture, and such ductile-brittle stripe patterns as shown in Fig. 7C were often observed. Since the spacing of the stripe patterns was similar to that of cellular dendrites, the flat, brittle-appearing regions were considered to correspond to the delta ferrite that was retained with skeletal morphology at the core of cellular dendrite, while the fringed ductile regions correspond to interdendritic austenite. This was supported by the fracture surface profiles. As shown in Fig. 8, the fracture of FA weld metal was extended preferentially in delta ferrite.

Figure 9 gives the nitrogen effect on the ultimate tensile strength (UTS) and 0.2% yield strength (0.2% YS) of the weld metal at 77 K. Increased nitrogen content increased both ultimate tensile and 0.2% yield strength. The degree of the nitrogen-strengthening effect was similar to that in the corresponding base metal (Ref. 3), although the yield strength of the weld metal was higher than that of the base metal. Delta-ferrite-containing weld metal (FA- and AF-mode weld metals) showed rather higher tensile and yield strength than fully austenitic weld metals. Ductility of the weld metal was comparable to or slightly lower than that of conventional 300-series weld metal, with elongation values ranging from 18 to 42% at a temperature of 77 K.

Figure 10 presents the strength-toughness trend at 77 K for the weld metal studied, indicating the inverse linear relationship between strength and toughness. It should be noted that the trend for the weld metal is toward inferiority in impact toughness compared to that for the corresponding base metal.

Hot Cracking Susceptibility

The results of the Varestraint test are shown in Table 3. Generally, the welds tested showed fairly low susceptibility compared with conventional 300-series welds, mainly due to extremely reduced sulfur and phosphorus contents. For instance, the total crack length of the most crack-susceptible, fully austenitic weld (No. 6) was one-third of that of the Type 310 weld and similar to that of the Type 316 weld.

Figure 11 gives the effect of nitrogen and solidification mode on the hot cracking susceptibility of the welds. Nitrogen had little effect on the susceptibility within each solidification mode. On the other hand, it was obviously indicated that fully austenitic, A-mode welds were the most susceptible, while primary ferrite solidification, FA mode was the most resistant

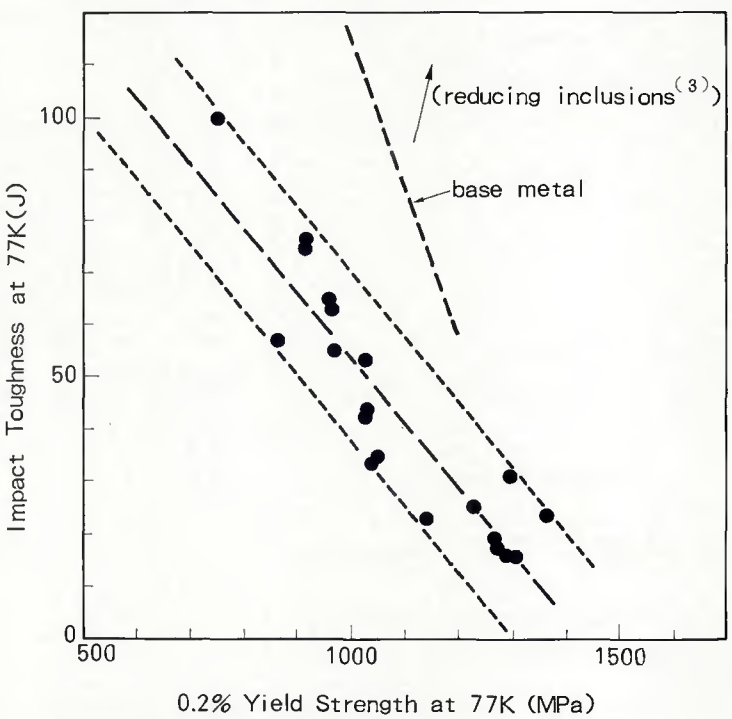

Fig. 10—Yield strength vs. impact toughness trend at 77 K for nitrogen-bearing austenitic stainless steel weld metals that were studied

Table 3—Varestraint Test Results

ID	Cr-Ni (wt-%)	Nitrogen Content[b] (wt-%)	Solidification Mode[b]	Ferrite Content (measured)[b] (%)	Total Crack Length (mm)
1	25-10	0.297	FA	6.6	0.1
2	25-11	0.318	FA	3.5	0.2
3	25-12	0.336	AF	2.3	0.6
4	25-13	0.345	AF	0.7	0.8
5	25-14	0.313	A	0	1.4
6	25-17	0.333	A	0	2.0
7	25-13	0.229	AF	2.8	0.5
8	25-14	0.167	FA	6.8	0.1
13	25-18	0.242	A	0	1.4
15	25-20	0.133	A	0	1.7
16	25-23	0.068	A	0	1.3
18[a]	25-20	0.368	A	0	1.5
19[a]	25-22	0.164	A	0	1.3
20[a]	25-23	0.245	A	0	1.5

(a) Newly melted heat for Varestraint test.
(b) Analyzed in as-tested weld.

to cracking, which is consistent with previous works (Refs. 23, 24). Note that, even if the weld solidifies as primary austenite, a ferrite-containing AF mode and extra-low impurity levels are beneficial in order to attain high resistance to hot cracking.

Discussion

Nitrogen Effect on Solidification Mode and Ferrite Number

The results obtained show that nitrogen content and metallurgical factors such as solidification mode and retained delta ferrite content of the weld metal influence the weld properties. Since both solidification mode and ferrite content are strongly affected by the nitrogen content in high-nitrogen weld metal, it is of great importance to evaluate the nitrogen effect on each in order to achieve desired weld properties. In the following sections, the nitrogen effect on such factors is discussed, assuming that other alloying elements such as carbon, silicon and manganese work in the same manner and degree as Schaeffler and DeLong predicted (Ref. 26), though there have been several objections as to the manganese effect (Refs. 6, 31, 32).

The classification of solidification modes of the weld metal makes it possible to evaluate the nitrogen effect on the mode as a nickel equivalent expression. Figure 12 shows the plots of the solidification mode on the coordinate of nitrogen content vs. DeLong's nickel equivalent value calculated without the nitrogen term. Note that both values are normalized by DeLong's chromium equivalent value (Cr_{eq}) to exclude the effect of variation of such ferritizers as chromium, silicon and molybdenum. The figure obviously indicates that increased nitrogen content and/or increased nickel content stabilize the austenite as the primary phase, thereby shifting the solidification mode from FA to A. On the plots, each solidification mode has a well-defined field, and the borders between the modes are given by solid and dotted lines. The border between FA and AF mode, given by the solid line, corresponds to the eutectic valley on the liquidus surface of the system studied. Therefore, the nitrogen effect on the primary phase is suggested as a nickel equivalent expression by the gradient of the line, which is approximately derived as 18. So, in order to describe the solidification mode of the weld metal, the nickel equivalent is modified by substituting the nitrogen coefficient of 18 in the DeLong nickel equivalent. Using the modified DeLong nickel equivalent (Ni'_{eq}), the border between FA and AF mode is given by the ratio $Cr_{eq}/Ni'_{eq} = 1.36$. If the Cr_{eq}/Ni'_{eq} ratio value calculated from the weld compositions is larger than 1.36, the weld metal solidifies as primary ferrite and ferritic solidification becomes more stable as the ratio value increases. On the

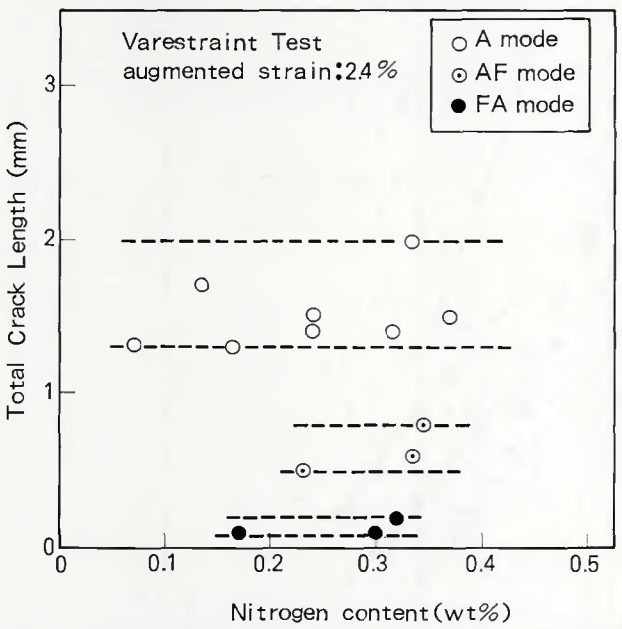

Fig. 11—Effect of nitrogen and solidification mode on hot cracking susceptibility of weld metal

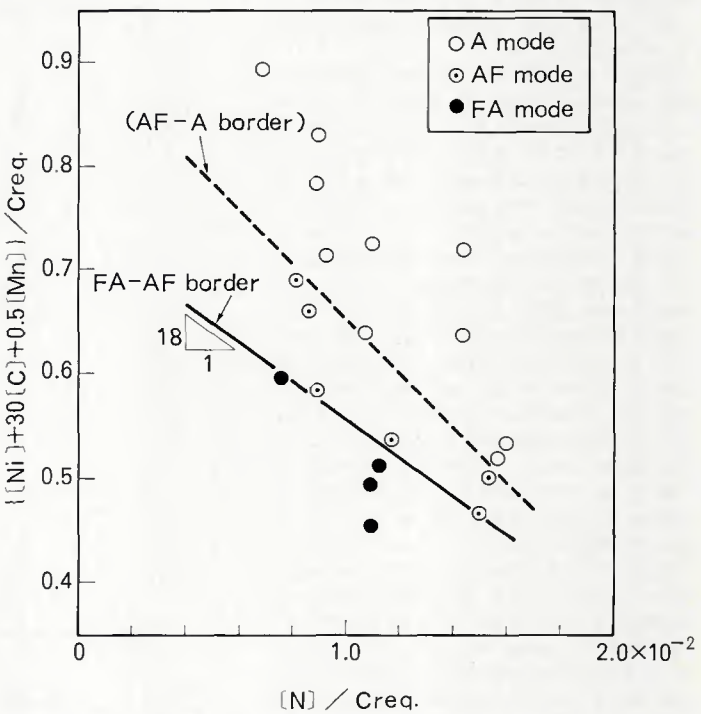

Fig. 12—Effect of nitrogen and other austenitizers on the weld solidification mode

contrary, if the ratio value is less than 1.36, the weld metal solidifies as the primary austenite, and austenitic solidification becomes more stable as the ratio value decreases, finally resulting in A mode at the value less than approximately 1.19. A mixed mode of FA and AF occurs at a value around 1.36.

As for the nitrogen effect on the weld ferrite content, different nitrogen coefficients for nickel equivalent expressions have been reported (Refs. 9, 26, 28, 29). Similar confusion has been experienced in manganese at higher content, and very recently Szumachowski and Kotecki (Ref. 32) offered an effective method to clarify the confusion. With reference to their method, the nitrogen effect on the weld ferrite content is evaluated. In the procedure, the nitrogen contribution to a nickel equivalent, ΔNi_{eq}, is derived so as to fit the actually measured ferrite content on the DeLong diagram for each ferrite-containing weld metal. As shown in Fig. 13, ΔNi_{eq} linearly increases with weld nitrogen, and the trend agrees with DeLong's prediction. Therefore, it is concluded that the nitrogen effect on the weld ferrite content is a linear function of weld nitrogen content, and the nitrogen coefficient of 30 is suitable to predict weld ferrite number from the weld compositions, even when the weld metals contain fairly large amounts of nitrogen. The ferrite number of the weld metal, calculated on the basis of the DeLong diagram, shows a good correlation with the measured ferrite content, as shown in Table 4.

Two different nitrogen coefficients, of 18 and 30, were obtained for the weld solidification mode and ferrite content, respectively. This suggests the different nitrogen effect as an austenitizer during and after solidification. The temperature dependency of the nitrogen effect has been pointed out by Suutala (Ref. 27), and, in addition, it can be expected through a simple thermodynamic consideration. Considering the free energy of nitrogen and nickel in iron for simplicity, the austenite-stabilizing effect of nitrogen for the nickel equivalent expression in iron can be given by $(\Delta^\circ G_N^{\alpha-\gamma Fe}/\Delta^\circ G_{Ni}^{\alpha-\gamma Fe}) \times (A_{Ni}/A_N)$, where $\Delta^\circ G_N^{\alpha-\gamma Fe}$ and $\Delta^\circ G_{Ni}^{\alpha-\gamma Fe}$ are the free energies of the reaction for nitrogen and nickel, respectively, when transferred from a solution in α iron to a solution in γ iron of the same composition, and A_N and A_{Ni} are the atomic weights of nitrogen and nickel, respectively. From calculations based on the previous studies (Refs. 33, 34), this value decreases as temperature increases. Extrapolating this result to the solidification temperature range, the trend agrees with the result obtained in the present study and Suutala's statement. This can be one of the possible explanations for the different nitrogen effect obtained, although the system discussed is too complicated to treat thermodynamically. From the standpoint of the solidification in the weld metal, the primary phase is determined by the composition of the first solid formed at the advancing cell or cellular dendrite tips. Though there have been several theoretical studies on the cell tip composition (Refs. 35, 36), if the solidification in the weld metals occurs simply under Case III condition (Ref. 37) to form cell or cellular dendrite, the first solid has the concentration of $k_X C_{o,X}$ for the element X, where k_X is the equilibrium partition ratio for the element X, and $C_{o,X}$ is the nominal concentration of the element X. The equilibrium partition ratio for nitrogen in steels has been reported as 0.3 to 0.5 (Refs. 38, 39), and this is smaller than that of 0.8 to 0.95 for other austenitizers such as nickel and manganese (Refs. 38, 39), which results in a relatively lower concentration of nitrogen in the first solid. As a consequence, the contribution of nitrogen to the primary phase formed at the cell or cellular dendrite tips is presumably smaller than that of nickel or manganese. On the other hand, as the temperature falls, a rather rapid diffusion rate of nitrogen in the solid accelerates the solid-state phase transformation from ferrite to austenite, and the larger nitrogen solubility in austenite increases the stability of austenite, both of which depend on the amount of nitrogen. Therefore, it can be concluded that the nitrogen effect as an austenitizer is stronger and more stable in the solid state than during solidification. This is also the case for carbon (Ref. 27). But the carbon content is very low in the weld metals studied; therefore, the difference of the carbon effect during and after solidification can be neglected in the present study.

Table 4—Calculated Ferrite Number (FN) of the Weld Metals Studied

Weld ID	Measured Ferrite Content (%)	Calculated FN (DeLong)
A1	8.8	8.0
A2	6.7	5.5
A3	5.2	3.5
A4	3.5	2.0
A5	0	−2.5
A6	0	−7.0
A7	3.0	4.0
A8	5.3	5.5
A9	1.2	0
A10	0	−1.0
A11	0	−4.0
A12	0	−9.0
A13	0	−7.0
A14	0	<−10.0
A15	0	−9.0
A16	0	−7.0
A17	0	<−10.0
N1	1.6	0
N2	0.5	−2.0
N3	0	−3.5
N4	0	−3.5
N5	0	−7.0
N6	0	<−10.0

Factors Influencing Weld Properties

Figure 14 shows the effect of calculated FN on the impact toughness and yield strength of the weld metal at 77 K (−320°F). The impact toughness tends to be degraded with the weld FN. Thus, increased FN is certainly detrimental to the impact toughness, as previous works have indicated (Refs. 17, 40), but the solidification mode and nitrogen content are found to be more influential factors for impact toughness over the FN range studied. On the other hand, the yield

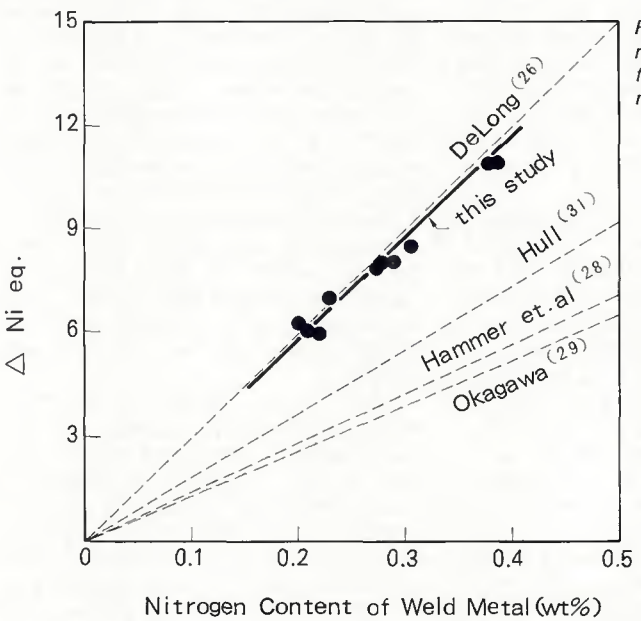

Fig. 13—ΔNi_{eq} vs. nitrogen content for the ferrite-containing weld metal

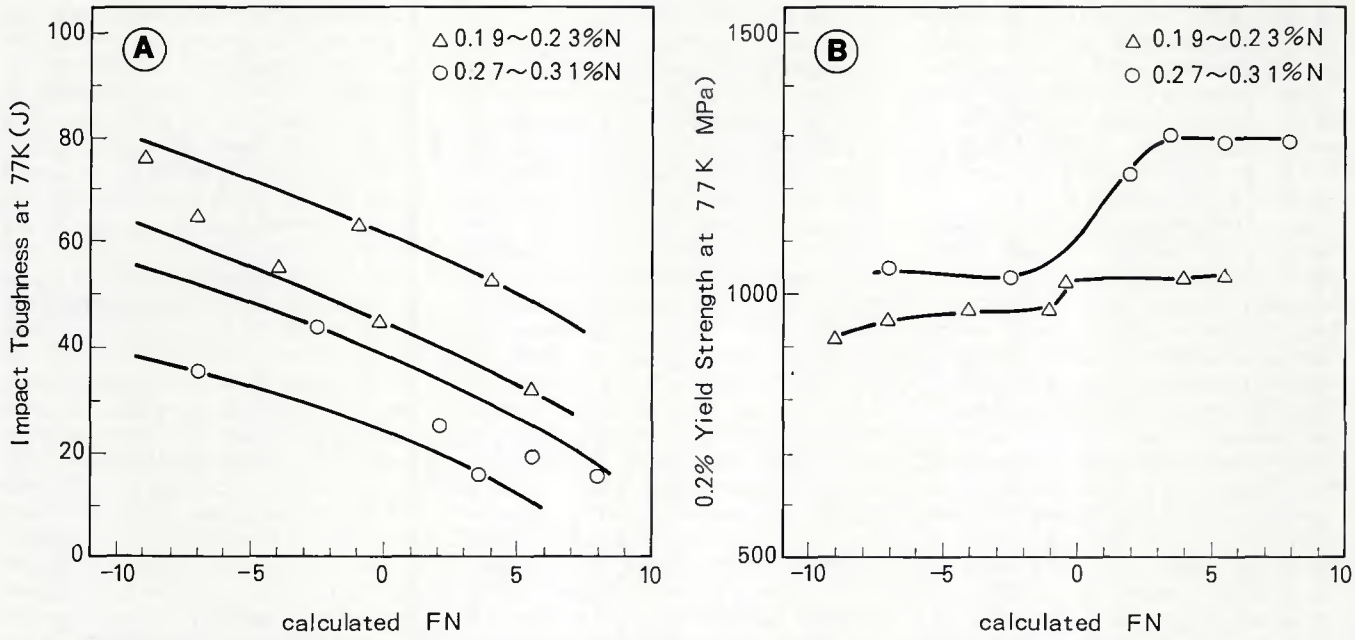

Fig. 14—Effect of ferrite number (FN) on the mechanical properties of weld metals at 77 K. A—Impact toughness; B—yield strength

strength of the weld metals increases dramatically around 0 FN.

As for the deleterious effect of ferrite on weld impact toughness, the morphology and distribution exert a major influence. Primary ferrite solidification mode leads to skeletal ferrite morphology with well-developed side branches in microstructure. It serves as a semicontinuous brittle phase at cryogenic temperature, thereby as a preferential path for fracture extension (Ref. 17). This was ascertained on the fracture surfaces and their profiles, as shown in Fig. 7C and Fig. 8C, respectively. On the other hand, the primary austenite solidification mode leads to little, if any, "vermicular" morphology of eutectic ferrite along the intercellular-dendritic regions in the microstructure, and such isolated ferrite morphology does not seem to affect impact toughness to a large extent even at cryogenic temperatures. In fact, few brittle-appearing regions were observed on the fracture surfaces for the AF-mode weld metal through the use of scanning electron microscopy.

Nitrogen exists either as a solid-solution strengthener or as a form of precipitates such as nitride and carbonitride in the weld metal. The former decreases the ductility of the matrix, particularly at cryogenic temperatures, and the latter provides the nucleation site for a microvoid in a ductile dimpling fracture, both of which consequently deteriorate weld toughness at cryogenic temperatures. Actually, the dimples on the fracture surfaces of high-nitrogen-containing weld metals tended to be smaller in size, due to more precipitations, compared to that of lower-nitrogen-containing weld metals. However, soluble nitrogen still exerts a major role on the degradation of impact toughness with nitrogen. This is suggested and supported by the tensile test result, which showed the yield strength of the weld metal at 77 K increased with nitrogen to the same degree as that of corresponding base metals. Strength of base metals is increased due to the strengthening effect of solid-solution nitrogen. Therefore, as to the nitrogen effect, it can be stated that both strength and toughness were controlled mainly by soluble nitrogen.

Weldments of Highly Nitrogen-Strengthened Austenitic Stainless Steel at 4 K (−452.5°F)

The results suggest the compositions and metallurgical factors of weld metal for cryogenic usage. From the standpoint of the impact toughness, primary austenite solidification mode is indispensable. The ferrite content, which is necessary to assure fissure-free welds, should be reduced to the lowest possible level close to 0 FN. Nitrogen content is to be determined considering the combination of impact toughness and strength. Generally, it should be reduced to some extent compared to that of the base metal, because strength of the weld metal is higher than that of the base metal, while the impact toughness is lower than that of base metal at the same nitrogen level.

Based on this, 30-mm (1.2-in.) thick nitrogen-strengthened austenitic stainless steel plates were welded with the proper filler metals. The welds exhibited no cracks or discontinuities, and excellent strength and toughness down to 4 K (−452.5°F), with a yield strength of 1370 MPa (198.6 ksi) and a fracture toughness of K_{IC} = 120 MPa/m at 4 K (Ref. 41).

Conclusions

The metallurgical factors and cryogenic properties of high-nitrogen austenitic stainless steel weld metals were investigated. Emphasis was placed on evaluating the effect of nitrogen on the metallurgical factors, such as the solidification mode and the ferrite number of the weld metal. Furthermore, the relationship between the metallurgical factors and weld properties were also investigated. The conclusions obtained in the present study are as follows:

1) Nitrogen behaves as an austenitizer in the weld metal.

2) The effect of nitrogen on the solidification mode of the weld metal is determined as the nitrogen coefficient of 18 for the nickel equivalent expression. Using the DeLong chromium equivalent (Cr_{eq}) and modified DeLong nickel equivalent (Ni'_{eq}), in which the nitrogen coefficient of 18 is employed, the solidification mode can be described by the Cr_{eq}/Ni'_{eq} ratio value. If the ratio value is more than 1.36, the weld metal shows a primary ferrite solidification mode, and if the ratio value is less than 1.36, the weld metal shows a primary austenite solidification mode. Mixed mode is obtained at the ratio value of around 1.36.

3) The effect of nitrogen on the ferrite number is the same as DeLong determined; therefore, the ferrite number of the high-nitrogen weld metal is predicted on the basis of the DeLong diagram, as well as the conventional 300-series austenitic stainless steel weld metal.

4) The difference of nitrogen coefficient in nickel equivalent for the solidification mode and ferrite number indicates that the nitrogen effect as an austenitizer

is small at the initial stage of solidification compared to the solid state after solidification.

5) Impact toughness of the weld metal at 77 K (−320°F) is degraded as the weld nitrogen content and/or ferrite number increased, and significantly deteriorated by the primary ferrite solidification mode. The deleterious effect of primary ferrite solidification mode is due to the semicontinuous ferrite morphology.

6) Both yield and tensile strengths of the weld metal at 77 K are markedly increased as the weld nitrogen increases. Ferrite content also improves the strength.

7) Hot cracking susceptibility of the weld metal is reduced by lowering the content of impurities. Nitrogen has little effect on susceptibility. Ferrite-containing welds are more resistant to hot cracking than fully austenitic welds, and the welds with the primary ferrite solidification mode are the most resistant.

References

1. Reed, R. P., and Simon, N. J. 1984. Low-temperature strengthening of austenitic stainless steels with nitrogen and carbon. *Advances Cryogenic Engineering Materials.* Vol. 30, A. F. Clark and R. P. Reed, eds., pp. 127–136, Plenum Press, N. Y.

2. McHenry, H. I. 1983. The properties of austenitic stainless steel at cryogenic temperatures. *Austenitic Steels at Low Temperature.* R. P. Reed and T. Horiuchi, eds., pp. 1–28, Plenum Press, N. Y.

3. Sakamoto, T., Nakagawa, Y., Yamauchi, I., Zaizen, T., Nakajima, H., and Shimamoto, S. 1984. Nitrogen-containing 25Cr-13Ni stainless steel as a cryogenic structural material. *Advances Cryogenic Engineering Materials.* Vol. 30, A. F. Clark and R. P. Reed, eds., pp. 137–144, Plenum Press, N. Y.

4. Yoshida, K., Nakajima, H., Koizumi, K., Shimada, M., Sanada, Y., Takahashi, Y., Tada, E., Tsuji, H., and Shimamoto, S. 1983. Development of cryogenic structural materials for Tokamak reactor. *Austenitic Steels at Low Temperatures.* R. P. Reed and T. Horiuchi, eds., pp. 29–40, Plenum Press, N. Y.

5. Morris, J. W., Jr., and Dalder, E. N. C. 1985. Cryogenic structural materials for superconducting magnets. *Journal of Metals* 37(10):24–33.

6. Brooks, J. A. 1975. Weldability of high N, high Mn austenitic stainless steel. *Welding Journal* 54(6):189-s to 195-s.

7. Ogawa, T., Aoki, S., Sakamoto, T., and Zaizen, T. 1982. The weldability of nitrogen-containing austenitic stainless steel: part 1—chloride pitting corrosion resistance. *Welding Journal* 61(5):139-s to 148-s.

8. Ogawa, T., Suzuki, K., and Zaizen, T. 1984. The weldability of nitrogen-containing austenitic stainless steel: part 2—porosity, cracking and creep properties. *Welding Journal* 63(6):213-s to 223-s.

9. Espy, R. H. 1982. Weldability of nitrogen strengthened stainless steels. *Welding Journal* 61(5):149-s to 156-s.

10. Espy, R. H. 1982. Evaluation of weld fillers to join nitrogen strengthened stainless steels for cryogenic applications (fusion and MHD energy). *Materials Studies for Magnetic Fusion Energy Applications at Low Temperatures—IV, NBSIR 81-1645,* R. P. Reed and N. J. Simon, eds., pp. 453–463, National Bureau of Standards, Boulder, Colo.

11. Lippold, J. C., and Savage, W. F. 1980. Solidification of austenitic stainless steel weldments: part 2—the effect of alloy composition on ferrite morphology. *Welding Journal* 59(2):48-s to 58-s.

12. Takalo, T., Suutala, N., and Moisio, T. 1979. Austenitic solidification mode in austenitic stainless steel welds. *Met. Trans. A* 10A(8): 1173–1181.

13. Suutala, N., Takalo, T., and Moisio, T. 1980. Ferritic-austenitic solidification mode in austenitic stainless steel welds. *Met. Trans. A* 11A(5):717–725.

14. David, S. A. 1981. Ferrite morphology and variations in ferrite content in austenitic stainless steel welds. *Welding Journal* 60(4): 63-s to 71-s.

15. Brooks, J. A., Williams, J. C., and Thompson, A. W. 1983. STEM analysis of primary austenite solidified stainless steel welds. *Met. Trans. A* 14A(1):23–31.

16. Brooks, J. A., Williams, J. C., and Thompson, A. W. 1983. Microstructural origin of the skeletal ferrite morphology of austenitic stainless steel welds. *Met. Trans. A* 14A(6): 1271–1281.

17. Read, D. T., McHenry, H. I., Steinmeyer, P. A., and Thomas, R. D., Jr. 1980. Metallurgical factors affecting the toughness of 316L SMA weldments at cryogenic temperature. *Welding Journal* 59(4):104-s to 113-s.

18. Grekula, A. I., Kujanpaa, V. P., and Karjalainen, L. P. 1984. Effect of solidification mode and impurities on pitting corrosion in AISI 316 GTA welds. *Corrosion* 40(11):569–572.

19. Lippold, J. C., and Savage, W. F. 1982. Solidification of austenitic stainless steel weldments: part 3—the effect of solidification behavior on hot cracking susceptibility. *Welding Journal* 61(12):388-s to 396-s.

20. Kujanpaa, V. P. 1985. Effects of steel type and impurities in solidification cracking of austenitic stainless steel welds. *Metal Construction* 17(1):40R to 46R.

21. Hull, F. C. 1967. Effect of delta ferrite on the hot cracking of stainless steel. *Welding Journal* 46(9):399-s to 409-s.

22. Lundin, C. D., DeLong, W. T., and Sponds, D. F. 1975. Ferrite-fissuring relationship in austenitic stainless steel weld metals. *Welding Journal* 54(8):241-s to 246-s.

23. Brooks, P. S., and Lambert, F. J., Jr. 1978. The effect of phosphorus, sulfur and ferrite content on weld cracking of type 309 stainless steel. *Welding Journal* 57(5):139-s to 143-s.

24. Cieslak, M. J., Ritter, A. M., and Savage, W. F. 1982. Solidification cracking and analytical electron microscopy of austenitic stainless steel weld metals. *Welding Journal* 61(1):1-s to 8-s.

25. Brooks, J. A., Thompson, A. W., and Williams, J. C. 1984. A fundamental study of the beneficial effects of delta ferrite in reducing weld cracking. *Welding Journal* 63(3):71-s to 83-s.

26. Long, C. J., and DeLong, W. T. 1973. The ferrite content of austenitic stainless steel weld metal. *Welding Journal* 52(6):281-s to 297-s.

27. Suutala, N. 1982. Effect of manganese and nitrogen on the solidification mode in austenitic stainless steel welds. *Met. Trans. A* 13A(12):2121–2130.

28. Hammar, O., and Svensson, U. 1979. Influence of steel composition on segregation and microstructure during solidification of austenitic stainless steels. *Solidification and Casting of Metals,* pp. 401–410, The Metal Society, London, England.

29. Okagawa, R. K., Dixon, R. D., and Olson, D. L. 1983. The influence of nitrogen from welding on stainless steel weld metal microstructures. *Welding Journal* 62(8):204-s to 209-s.

30. Bennett, F. W., and Dillon, C. P. 1966. Impact strength of austenitic stainless steel welds at −320°F—effects of composition, ferrite content and heat-treatment. *Journal of Basic Engineering* 88:3.

31. Hull, F. C. 1973. Delta ferrite and martensite formation in stainless steels. *Welding Journal* 52(5):193-s to 203-s.

32. Szumachowski, E. R., and Kotecki, D. J. 1984. Effect of manganese on stainless steel weld metal ferrite. *Welding Journal* 63(5):156-s to 161-s.

33. Hillert, M., Wada, T., and Wada, H. 1967. The α–γ equilibrium in Fe-Mn, Fe-Mo, Fe-Ni, Fe-Sb, Fe-Sn and Fe-W system. *JISI* 205(5):539–546.

34. Agren, J. 1979. A thermodynamic analysis of the Fe-C and Fe-N phase diagrams. *Met. Trans. A* 10A(12):1847–1852.

35. Burden, M. H., and Hunt, J. D. 1974. Cellular and dendrite growth. *J. Cryst. Growth* 22:109–116.

36. Flemings, M. C. 1974. *Solidification Processing,* p. 79, McGraw-Hill, N.Y.

37. Lippold, J. C., and Savage, W. F. 1979. Solidification of austenitic stainless steel weldments: part 1—a proposed mechanism. *Welding Journal* 58(12):362-s to 374-s.

38. Chipman, J. 1951. *Physical Chemistry of Steelmaking Committee, Iron and Steel Division, AIME,* p. 632, American Institute of Mining and Metallurgical Engineering.

39. Sims, C. E. 1962. *Electric Furnace Steelmaking,* Vol. 2, p. 99, John Wiley & Sons.

40. Szumachowski, E. R., and Reid, H. F. 1978. Cryogenic toughness of SMA austenitic stainless steel weld metals: part 1—role of ferrite. *Welding Journal* 57(11):325-s to 333-s.

41. Nakajima, H. Private communication.

42. Read, D. T., and Reed, R. P. 1981. Fracture and strength properties of selected austenitic stainless steels at cryogenic temperatures. *Cryogenics* 21(6):415–417.